ELSEVIER

Journal of Biomechanics 35 (2002) 517–521

JOURNAL OF BIOMECHANICS

www.elsevier.com/locate/jbiomech
www.JBiomech.com

Technical note

Measurement of a spinal motion segment stiffness matrix

Ian A. Stokes[a,*], Mack Gardner-Morse[a], David Churchill[b], Jeffrey P. Laible[c]

[a] *Department of Orthopaedics and Rehabilitation, University of Vermont, Burlington, VT 05405, USA*
[b] *Department of Neurology, University of Vermont, Burlington, VT 05405, USA*
[c] *Department of Civil and Environmental Engineering, University of Vermont, Burlington, VT 05405, USA*

Accepted 29 September 2001

Abstract

The six-degrees-of-freedom elastic behavior of spinal motion segments can be approximated by a stiffness matrix. A method is described to measure this stiffness matrix directly with the motion segment held under physiological conditions of axial preload and in an isotonic fluid bath by measuring the forces and moments associated with each of the six orthogonal translations and rotations. The stiffness matrix was obtained from the load–displacement measurements by linear least squares assuming a symmetric matrix. Results from a pig lumbar spinal motion segment in an isotonic bath, with and without a 500 N axial preload, showed a large stiffening effect with axial preload.

Keywords: Spine; Stiffness; Motion segment; Flexibility; Joint mechanics

1. Introduction

The linearized elastic behavior of spinal motion segments (two vertebrae and the intervening facet joints, disc and ligaments) was described in 1976 by Panjabi et al. (1976) with a stiffness matrix that was obtained experimentally by inverting a flexibility matrix. In general, the stiffness matrix has 36 independent coefficients. Using conservation of energy and the assumption of linear elastic materials the matrix is symmetric. This reduces the number of independent coefficients to 21. Motion segment stiffness matrices and derived equivalent beam representations (Gardner-Morse et al., 1990) have been used in simulations of surgery (Stokes and Gardner–Morse, 1993), analyses of spinal force equilibrium (Stokes and Gardner-Morse, 1995), and stability analyses (Gardner-Morse et al., 1995).

There are several limitations of the existing experimentally derived stiffness data. Most reported data were obtained without compressive preload. The only complete published stiffness matrix (for thoracic motion segments) (Panjabi et al., 1976) was obtained indirectly by inversion of a flexibility matrix. Motion segment load–displacement properties are nonlinear (Panjabi et al., 1989), and when a physiological axial preload is applied several terms of the stiffness matrix have been found to increase by a factor of 2 or more (Edwards et al., 1987; Janevic et al., 1991; Panjabi et al., 1977). Preload may also reduce the amount of nonlinearity (Janevic et al., 1991). The alteration in stiffness with preload is associated with both intervertebral disc and facet joint properties (Janevic et al., 1991) and this effect was predicted analytically in a model of the disc that includes geometrical effects of large disc compression and nonlinear elastic tissue properties (Broberg, 1983). Experiments with preload are complicated by associated moments that are altered by displacements of the point of preload application (Cripton et al., 2000; Edwards et al., 1987). Patwardhan et al. (1999) present an empirical 'follower load' method to maintain approximately pure axial loading on a multi-motion-segment section of the spine while it displaces. To address such geometrical nonlinearity in a flexibility experiment, Edwards et al. (1987) resolved sagittal plane loads applied to the specimen into two forces and a moment, taking finite displacements into account. Then, a least-squares method was used to determine the stiffness coefficients in each degree of freedom, for both high and low magnitude forces because the stiffnesses were not constant. The stiffness method controls the

*Corresponding author. Tel.: +1-802-656-2250; fax: +1-802-656-4247.
E-mail address: Ian.Stokes@uvm.edu (I.A. Stokes).

0021-9290/02/$ - see front matter
PII: S0021-9290(01)00221-4

displacements of the preloaded specimen and avoids potential instability of a test specimen.

The load–displacement relationship is also time dependent, and this effect is attributed to viscoelastic, osmotic and poroelastic effects. Pflaster et al. (1997) has demonstrated that discs in a physiological saline bath have greater hydration than discs that are just exposed to a saline spray and wrap. This increased hydration presumably affects the mechanical properties of discs.

Based on these considerations a method was developed to measure motion segment stiffness directly under testing conditions that simulate physiological conditions, including axial preload and with the specimen immersed in an isotonic fluid bath.

2. Methods

A testing machine was constructed in the form of a 'Steward platform' or 'hexapod' robot (Fig. 1). It consisted of a moving platform supported by six linear actuators mounted to a stationary base. The platform could be driven to any six-degree-of-freedom (6-DOF) position by controlling the actuator lengths. The actuators were constructed from stepper motors (Oriental Motor USA Corp., Torrance, CA, USA), coupled to precision lead screws (Ball Screws and Actuators Co., Inc., San Jose, CA, USA) and custom Teflon nuts.

A 6-DOF load cell (MC3A-6-500, Advanced Mechanical Technology Inc., Waltham, MA, USA) was mounted below the moving platform (see Fig. 1). The load cell had been calibrated to provide a sensitivity matrix (taking crosstalk into account), and had linearity and hysteresis better than 0.2% of full-scale output. A specimen mounting plate was fixed to the lower (live) side of this loadcell. Test specimens were installed in the machine with one end fastened to the specimen mounting plate and the other end fastened to the base pedestal. The pedestal incorporated a transparent plexiglass bath for immersing the specimen in circulating isotonic saline cooled to approximately 4°C.

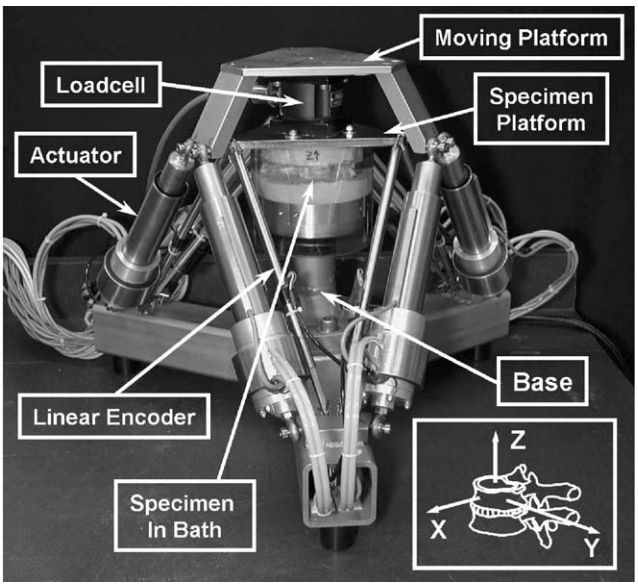

Fig. 1. Photograph of the hexapod apparatus showing actuators, base pedestal, specimen mounting plate, linear encoders, moving platform, loadcell and lumbar motion segment specimen that can be seen through the transparent bath surrounding it. Inset: the axis system convention.

Six linear encoders were used to measure and control the displacements of the testing machine. These incorporated glass scales and optical read heads providing 2.54 μm resolution (Model LDK, Dynamics Research Corp., Wilmington, MA, USA). Each scale contained a reference mark that allowed the encoders to report absolute length once the appropriate 'homing' sequence was performed on system startup. The encoders were mounted nominally parallel to the actuators, but were not physically linked to them. Instead, they spanned between the stationary base, and the specimen mounting plate. Therefore, they provided a measure of the true position of the specimen mounting plate independent of loadcell compliance or drivetrain backlash, analogous to using a specimen-mounted extensometer in uniaxial testing.

A six-axis motion controller (DMC-1860, Galil Motion Control, Inc., Rocklin, CA, USA) drove the Steward platform's motions under closed-loop position control. Position feedback was provided by the six linear encoders. For any desired position of the specimen mounting plate, the required lengths of the six encoders were calculated using vector-loop algebra. The control system then drove the actuators such that the encoders reached these lengths. Length changes were programmed to produce rotations and translations about any arbitrary axis system. The motion controller was installed in a Pentium class PC computer. The motion controller's six channel 16-bit A/D converter also read the analog signals from the load cell. A custom written software package running in LabView (version 5.1, National Instruments, Austin, TX, USA) provided an interface allowing the user to define desired motions, and to collect specimen load and displacement data. The accuracy of the positional control was verified by using a pair of dial indicators (B.C. Ames Co., Waltham, MA, USA) accurate to 2.54 μm.

The test specimen was a pig lumbar spinal motion segment consisting of two vertebrae and the intervening soft tissue. Surrounding muscles were removed leaving the ligaments intact. Three screws were driven into each vertebra, which were then embedded in PMMA in end-fittings that bolted rigidly to the

testing machine, using a jig to align the specimen's axis with the parallel end-fittings. The axis system chosen for initial experiments was an ISO axis system (Fig. 1) located at the center of the superior vertebral body and aligned with the anatomical planes (Stokes et al., 1994), as identified on biplanar radiographs of the embedded specimen. An axial compressive preload of 500 N (representing typical active in vivo quadruped loading (Hauerstock et al., 2001) was applied and the specimen was allowed to equilibrate with this force for 3 h. When a specimen was left overnight (15 h) to re-equilibrate from the 500 N preload condition to the zero preload condition, 90% of the recovery from axial compression occurred after the first 2.5 h. Six pure displacement tests (three translations and three rotations) were then sequentially performed while the six encoder lengths and the six load components were recorded at 2 Hz. The specimen was left unloaded overnight, and thenthe six displacement tests were repeated. Each displacement test consisted of five cycles in which the position was ramped at a constant rate between a minimum and maximum value (sawtooth waveform). The displacements were ± 3 mm along the X-axis, ± 1.5 mm along the Y-axis, ± 0.4 mm along the Z-axis and $\pm 4^\circ$ about each axis. These ranges were selected to represent typical physiological ranges of displacements and forces. Each cycle of translation or rotation took 174 s to complete, at which speed tests could be monitored visually to avoid specimen injury. The actuators of the present apparatus have a maximum (unloaded) velocity of 76 mm/min. At slower speeds in an intermediate position of the specimen mounting plate under typical combined loadings, the maximum forces exceed 350 N in shear and 1100 N in the Z-direction (which can be augmented by deadweights). The maximum Z-axis moment exceeds 10 N m and the other moments exceed 35 N m.

In post-processing, the forces and moments at the vertebral body center were calculated from the loadcell recordings by a rigid body transformation and the actual displacements of the center of the superior vertebral body were calculated from the six recorded encoder lengths using the testing machine geometry. Operation of the testing machine was verified during a zero preload experiment by examining the measured out-of-plane displacements (e.g. when a Y-translation was applied, the X-translation, Z-translation and the 3 rotations should be nominally zero).

The loads and displacements were considered to be related by the linear relationship with a symmetric stiffness matrix

$$[K]\{X\} + \{F_0\} = \{F\}, \tag{1}$$

where $[K]$ is a 6×6 stiffness matrix with 36 coefficients (21 independent coefficients due to symmetry), $\{X\}$ is a 6×1 displacement vector of 3 translations followed by the three rotations, $\{F_0\}$ is a 6×1 initial offset load vector (three forces and three moments), and $\{F\}$ is a 6×1 load vector of the three resulting forces and three resulting moments. This equation can be rearranged into the standard least squares form for the stiffness coefficients and initial offset load

$$[D \vdots I]\begin{Bmatrix} k \\ \dots \\ F_0 \end{Bmatrix} = \{F\}, \tag{2}$$

where $[D]$ is a 6×21 matrix based on the six displacements in $\{X\}$, $[I]$ is a 6×6 identity matrix and $\{k\}$ is a 21×1 vector of the 21 independent stiffness coefficients in $[K]$. By using the data from the six orthogonal displacement trials with redundant measurements, Eq. (2) can be solved using linear least squares (Lawson and Hanson, 1974) for the stiffness coefficients. This equation is a three-dimensional extension and generalization of the least-squares method given in Edwards et al. (1987). The coefficient of determination (R^2) was calculated for the linear least-squares estimates.

3. Results

When the pure single axis translations or rotations were imposed on the specimen, the greatest recorded displacements in other directions were 8 μm and 0.004° indicating that the amount of displacement 'crosstalk' in the testing apparatus was close to the theoretical limit due to the encoder resolution of 2.54 μm.

Each of the single displacement tests produced data like those presented in Figs. 2 and 3. The degree of linearity, hysteresis and repeatability of the load–displacement behavior over the five cycles in each trial can be seen in these figures. Creep behavior influenced the ability to maintain preload. During the test with 500 N preload the axial compression was increased by 0.98 mm to maintain the 500 N axial load, even after the specimen had been left for 3 h to equilibrate to this axial load.

In these preliminary experiments, it was found that there was a several fold increase in the stiffness matrix terms with a 500 N axial preload applied (Table 1). Also, the linearity of the load–displacement relationships was greater in the tests with 500 N axial preload, as evidenced by the overall R^2 values for stiffness matrix fits to the experimental data of 0.80 and 0.72 with and without preload, respectively.

4. Discussion

This methodology was found to be an efficient and direct way to obtain the load–displacement properties

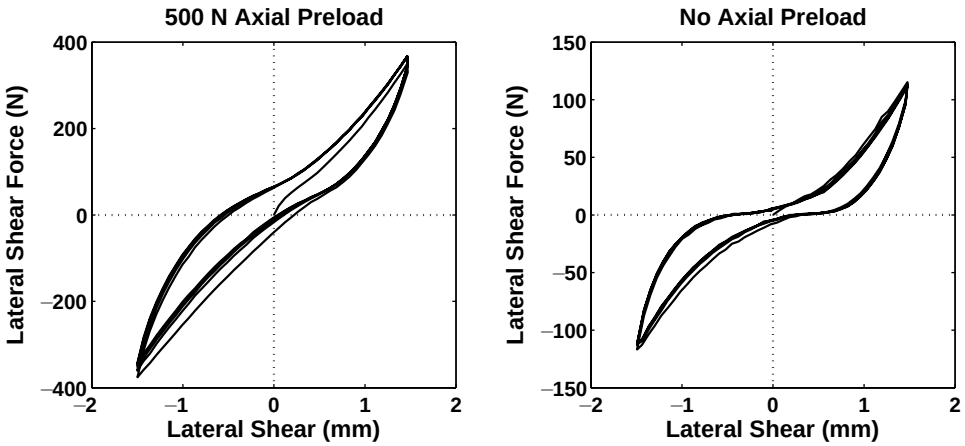

Fig. 2. Graph of Y (lateral) force produced by Y-translation (left) with 500 N axial preload and (right) without axial preload, for five cycles of 'sawtooth' displacement. Note that the input displacement was the same for both preload conditions, but the resulting forces differed by a factor of approximately three.

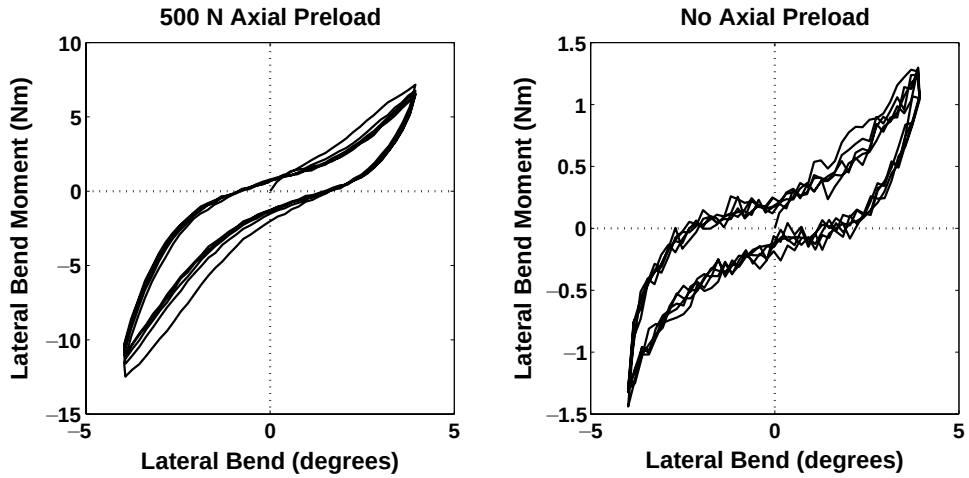

Fig. 3. Graph of the X (lateral bend) moment produced by rotation about the X-axis (left) with 500 N axial preload and (right) without axial preload, for five cycles of 'sawtooth' rotation. Note that the input rotation was the same for both preload conditions, but the resulting moments differed by a factor of approximately seven.

Table 1
Terms of the least-squares estimated symmetric stiffness matrix for a pig motion segment (obtained using Eq. (1))

Preload (N)	T_x	T_y	T_z	R_x	R_y	R_z	
500	108	−6	125	381	−1630	−29	F_x
0	35	3	11	45	−623	−87	
500		190	15	2490	396	−2390	F_y
0		49	−1	702	−10	−526	
500			2080	4060	6770	−36	F_z
0			67	41	150	50	
500				98,800	19140	−44,400	M_x
0				11,500	−273	−10,400	
500		Symmetric			105,000	−7070	M_y
0					13,300	3320	
500						115,000	M_z
0						35,400	

For each of the terms in the matrix, the values from a test with 500 N axial preload and a test with zero preload are given. Each term is the derived relationship between a displacement component and a load component. T_x, T_y, T_z refer to translations, R_x, R_y, R_z refer to rotations, and F_x, F_y, F_z, M_x, M_y, M_z are the associated forces and moments. Units are N, mm and rad.

of a motion segment under physiological conditions of axial preload and in a physiological fluid medium. The six actuator testing machine allowed the specimen to be rigidly mounted and contained in a isotonic saline bath during testing. The direct measurement of a stiffness matrix avoided errors in inverting a linearized flexibility matrix that might be ill-conditioned.

Errors in the terms of the stiffness matrix could arise from specimen misalignment during embedding, nonlinearity, rate dependencies, hysteresis and creep in the force–displacement relationships. Although care was taken to minimize embedding errors, it was assumed that the testing axes coincided with the local axis system for the motion segment. The rotation axes were set at the superior vertebral body center, to obtain a stiffness matrix referred to this point. In a preliminary test, rotations were subsequently applied at the disc center, and a rigid offset correction was applied to derive a stiffness matrix for the vertebral body center. The diagonal terms of the two independently derived stiffness matrices agreed to within 10%, which was comparable with the observed test–retest repeatability.

By assuming symmetrical behavior about the sagittal plane, the number of stiffness coefficients in the least–squares estimation could have been reduced from 21 to 12 (e.g. lateral shear forces associated with flexion and extension rotations would be assumed to be zero). Such terms were observed to be relatively small in Table 1. Because of the high stiffness in axial compression and the relatively low rotation stiffness about the X- and Y-axis, the interactions between these degrees of freedom are expected to be the most sensitive to embedding errors. The linear stiffness matrix is inevitably an approximation to the true load–displacement behavior, but it can be obtained directly from these experiments, and can then be employed in linear biomechanical analyses. Although it appears that the motion segment behavior was more linear with 500 N preload, nonlinearity and time dependence remain. The raw data from this apparatus could ultimately be used to fit a more complex model, including elastic nonlinearity and time-dependent behavior.

The stiffness was observed to increase with addition of the 500 N axial preload as has been reported in other studies (Edwards et al., 1987; Janevic et al., 1991; Panjabi et al., 1977). This implies that analyses of the spine that simulate in vivo loading conditions should take this effect into account. Similarly, it suggests that studies of motion segment stiffness without preload underestimate the true in vivo values.

Acknowledgements

This work supported by National Institutes of Health Grant R01 AR 44119. The authors thank Galil Motion Control, Inc. for their partial contribution of the motion control board, Dr. Jean-Guy Beliveau for helpful ideas and discussions about analytical methods and Dr. Donita Bylski-Austron for help in obtaining porcine test specimens.

References

Broberg, K.B., 1983. On the mechanical behaviour of intervertebral discs. Spine 8, 151–165.

Cripton, P.A., Bruehlmann, S.B., Orr, T.E., Oxland, T.R., Nolte, L.-P., 2000. In vitro axial preload application during spine flexibility testing: towards reduced apparatus-related artefacts. Journal of Biomechanics 33 (12), 1559–1568.

Edwards, W.T., Hayes, W.C., Posner, I., White, A.A., Mann, R.W., 1987. Variation of lumbar spine stiffness with load. Journal of Biomechanical Engineering 109, 35–42.

Gardner-Morse, M.G., Laible, J.P., Stokes, I.A.F., 1990. Incorporation of spinal flexibility measurements into finite element analysis. Journal of Biomechanical Engineering 112, 481–483.

Gardner-Morse, M., Stokes, I.A.F., Laible, J.P., 1995. Role of muscles lumbar spine stability in maximum extension efforts. Journal of Orthopaedic Research 13 (5), 802–808.

Hauerstock, D., Reindl, R., Steffen, T., 2001, Telemetric measurement of compressive loads in the sheep lumbar spine. In: Transactions of the 47th Annual Meeting of the Orthopaedic Research Society, San Francisco, CA, Abstract No.0931. http://www.ors.org/secure/47/pdfs/0931.pdf

Janevic, J., Ashton-Miller, J.A., Schultz, A.B., 1991. Large compressive preloads decrease lumbar motion segment flexibility. Journal of Orthopaedic Research 9 (2), 228–236.

Lawson, C.L., Hanson, R.J., 1974. Solving Least Squares Problems. Prentice-Hall, Englewood Cliffs, NJ, pp. 1-73.

Panjabi, M.M., Brand, R.A., White, A.A., 1976. Three-dimensional flexibility and stiffness properties of the human thoracic spine. Journal of Biomechanics 9, 185–192.

Panjabi, M.M., Krag, M.H., White, A.A., Southwick, W.O., 1977. Effects of preload on load displacement curves of the lumbar spine. Orthopedic Clinics of North America 8, 181–192.

Panjabi, M., Abumi, K., Duranceau, J., Oxland, T., 1989. Spinal stability and inter-segmental muscle forces: a biomechanical model. Spine 14, 194–200.

Patwardhan, A.G., Havey, R.M., Meade, K.P., Lee, B., Dunlap, B., 1999. A follower load increases the load-carrying capacity of the lumbar spine in compression. Spine 24 (10), 1003–1009.

Pflaster, D.S., Krag, M.H., Johnson, C.C., Haugh, L.D., Pope, M.H., 1997. Effect of test environment on intervertebral disc hydration. Spine 22 (2), 133–139.

Stokes, I.A.F. (chair), 1994. Scoliosis Research Society Working Group on 3-D terminology of spinal deformity: three-dimensional terminology of spinal deformity. Spine 19, 236–248.

Stokes, I.A.F., Gardner–Morse, M., 1993. Three–dimensional simulation of Harrington distraction instrumentation for surgical correction of scoliosis. Spine 18, 2457–2464.

Stokes, I.A.F., Gardner-Morse, M., 1995. Lumbar spine maximum efforts and muscle recruitment patterns predicted by a model with multijoint muscles and flexible joints. Journal of Biomechanics 28 (2), 173–186.